Molecular Therapy
Oncolytics
Original Article

Cetuximab-Triptolide Conjugate Suppresses the Growth of EGFR-Overexpressing Lung Cancers through Targeting RNA Polymerase II

Keqiang Zhang,[1,4] Yuelong Ma,[2,4] Yuming Guo,[3] Ting Sun,[1] Jun Wu,[3] Rajendra P. Pangeni,[1] Min Lin,[2] Wendong Li,[1] David Horne,[2] and Dan J. Raz[1]

[1]Division of Thoracic Surgery, City of Hope National Medical Center, Duarte, CA, USA; [2]Department of Molecular Medicine, City of Hope National Medical Center, Duarte, CA, USA; [3]Division of Comparative Medicine, City of Hope National Medical Center, Duarte, CA, USA

To overcome poor pharmacokinetics and toxicity of triptolide (TPL), a natural compound that exhibits potent anticancer activities, we developed a novel antibody-drug conjugate (ADC) to specifically deliver TPL to epidermal growth factor receptor (EGFR)-overexpressing non-small cell lung cancer (NSCLC) and others. The ADC (Cet-TPL) is made by conjugation of TPL to lysine residues of cetuximab (Cet), a clinically available anti-EGFR monoclonal antibody. Studies of antitumor efficacy demonstrated that Cet-TPL drastically suppressed *in vitro* proliferation and *in vivo* growth of these EGFR-overexpressing cancers, including NSCLC A549 and H1299 cells and two patient-derived xenografts, and head and neck squamous carcinoma UM-SCC6 cell, while it did not inhibit the proliferation and growth of NSCLC H520 that rarely expresses EGFR. Furthermore, immunofluorescence analysis revealed that Cet-TPL was effectively internalized and transported into lysosomes of EGFR-overexpressing cells. Cet-TPL effectively led to degradation of RNA polymerase II (Pol II) and demethylation of histone H3 lysines, and significantly induced apoptosis in these EGFR-overexpressing cancers. Compared with TPL, Cet, or their combination, Cet-TPL displayed higher target-specific cytotoxicity against EGFR-expressing cancers and much lower *in vivo* toxicity. In addition, Cet-TPL efficiently suppressed the activated EGFR pathway in UM-SCC6 cancer cells. Taken together, Cet-TPL represents a potent targeting therapeutic agent against EGFR-overexpressing NSCLC and others.

INTRODUCTION

Lung cancer is the leading cause of cancer-related deaths worldwide.[1] The two predominant non-small cell lung cancer (NSCLC) histological phenotypes are adenocarcinoma (~50%) and squamous cell carcinoma (~40%).[1] KRAS and epidermal growth factor receptor (EGFR) mutations are the most frequent oncogenic drivers discovered in lung adenocarcinomas. For lung squamous cell carcinoma, genes such as fibroblast growth factor receptors 1–3 (FGFR1–3) and genes in the phosphoinositide 3-kinase (PI3K) pathway seem to be more commonly mutated in lung squamous carcinoma.[2,3] Many targeted therapies against kinases EGFR, anaplastic lymphoma kinase (ALK), and c-Ros oncogene 1 receptor tyrosine kinase (ROS1) have been developed with compelling clinical proofs of concept and various survival benefits; however, treatment responses are typically short-lived.[2,3] Several KRAS-targeted therapies are under investigation, but none is currently approved for clinical use. Despite advances in targeted therapies and immunotherapy, most lung cancers are still incurable, and the 5-year survival rate for NSCLC patients remains only 15%; therefore, new therapies are urgently needed.[4]

Triptolide (TPL) is a natural compound isolated from the Thunder God Vine, *Tripterygium wilfordii*,[5] which has been used in traditional Chinese medicine to treat autoimmune disorders and inflammation,[6] including lupus[7] and rheumatoid arthritis.[8] TPL has shown antitumor activity in a variety of cancers, including lung cancer. TPL perturbs multiple signaling pathways, including NF-κB (nuclear factor kappa-light-chain-enhancer of activated B cells),[9] heat shock protein 70 (HSP70),[10] BCL-2,[11] and p53 pathways,[12] and through these signaling pathways TPL decreases cell proliferation and induces apoptosis. Recently, a study reported that TPL covalently binds to human XPB, a subunit of the transcription factor TFIIH, and inhibits its DNA-dependent ATPase activity that leads to the inhibition of RNA polymerase II (Pol II)-mediated transcription,[13,14] which may account for the majority of the known biological activities and molecular mechanism of action of TPL and be an explanation to many of its therapeutic properties, including its robust and promising anticancer properties. In lung cancer, TPL has been shown to sensitize cells to TRAIL-induced apoptosis and enhance p53 activity.[15] We previously showed that treatment with TPL and its derivative led to decreased lung cancer cell growth, invasion, and metastasis.[16–18] Despite its

Received 16 April 2020; accepted 1 July 2020;
https://doi.org/10.1016/j.omto.2020.07.001.

[4]These authors contributed equally to this work.

Correspondence: Dan J. Raz, MD, MS, Division of Thoracic Surgery, City of Hope National Medical Center, Duarte, CA, USA.
E-mail: draz@coh.org
Correspondence: David Horne, PhD, Department of Molecular Medicine, City of Hope National Medical Center, Duarte, CA, USA.
E-mail: dhorne@coh.org

great promise as an anticancer drug in preclinical models, its clinical use is limited by its toxicity and unfavorable pharmacokinetics, including poor water solubility.[19,20] Recently, TPL derivatives have been developed in order to optimize its bioavailability and decrease its toxicity. Minnelide, a TPL derivative, is currently in a phase II study in metastatic pancreatic cancer and is given as a daily infusion (ClinicalTrials.gov: NCT03117920).[21] Another TPL derivative, MRx102, has shown excellent anticancer effects in lung cancer and leukemia in animal models with minimal toxicity.[18,22]

Therapeutic antibodies have been proved an efficacious drug modality for their easy generation, specificity, and bio-durability. One strategy to reduce the toxicity of TPL is to deliver it selectively to tumor cells over their normal counterparts. EGFR is overexpressed on the cell surface in most lung cancers,[23] and it is also commonly overexpressed in many cancers, including head and neck, breast, colon, ovarian, and cervical cancers, suggesting that anti-EGFR antibody may be useful to deliver TPL to a variety of cancer types.[24–27] Cetuximab (Cet) is an anti-EGFR antibody approved for treatment of head and neck and colon cancers.[28] Here, we report a novel antibody-drug conjugate (ADC) that is built by conjugating TPL to the humanized anti-EGFR monoclonal antibody (mAb) Cet (Cet-TPL), which may specifically bind to the EGFR on cancer cells to deliver TPL. We have tested this conjugate in lung cancer cell lines, as well as in several mouse xenograft models of lung cancers and head and neck cancers. We have found that Cet-TPL has potent anticancer activity against EGFR-overexpressing cancer growth via the degradation of Pol II subunit POLR2A of the TFIIH complex, one of the general transcription factors for Pol II, and leads to multiple histone H3 lysine demethylation. Compared with TPL, Cet, or their combinations, Cet-TPL displays higher target-specific cytotoxicity against EGFR-expressing cancers and much lower *in vivo* systemic toxicity. In addition, Cet-TPL also efficiently suppresses the activated EGFR pathway in UM-SCC6 head and neck squamous carcinoma cell. Taken together, Cet-TPL represents a potential targeted therapeutic agent against EGFR-overexpressing NSCLC and other cancers.

RESULTS

Characteristic Analysis of Cet-TPL Conjugates

Schematic of chemical conjugation of Cet with TPL is shown in Figures 1A and 1B. Figure 1C shows results of a sodium dodecyl sulfate-polyacrylamide gel electrophoresis (SDS-PAGE) of Cet and Cet-TPL. The samples were loaded with Laemmli sample buffer with or without 2-mercaptoethanol (2-ME) as marked. Figure 1D shows the mass results of the fast protein liquid chromatography (FPLC) purified Cet-TPL after deglycosylation and reduction into the heavy chain and the light chain. Based on the relative abundance of the mass peaks, an average of about 5.5 TPLs per Cet was calculated.

In Vitro Cytotoxicity of Cet-TPL to EGFR-Overexpressing Cancer Cells

To examine the antitumor efficacy of Cet-TPL, we first examined its cytotoxicity to EGFR-expressing cancer cells compared with free TPL. As shown in Figure 2A, western blot analysis reveals that EGFR is highly expressed in the head and neck squamous carcinoma UM-SCC6 cells and NSCLC A549 and H1299 cells, but not in NSCLC H520 cells. The proliferation assays showed that TPL significantly suppressed the *in vitro* proliferation of all cancer cells in a dosage-dependent manner (Figure S1), whereas Cet alone did not inhibit the *in vitro* proliferation of A549 (Figure 2B), H1299 (Figure 2C), and H520 (Figure 2D), except for the proliferation of UM-SCC6 cells (Figure 2E), indicating the EGFR signaling pathway plays a crucial role only in cellular proliferation of UM-SCC6 cells. Compared with the control (immunoglobulin G [IgG]) and Cet, Cet-TPL displayed a dosage-dependent cytotoxic effect on all of these EGFR-expressing cancer cells A549, H1299, and UM-SCC6, except for H520, which does not express detectable EGFR (Figures 2B–2E), suggesting that Cet-TPL is specific for EGFR-expressing cancer cells. Also, based on the ratio of half-maximal inhibitory concentration (IC_{50}) of TPL to the conjugate of H520 (arbitrary index = 40) and that of H1299 (arbitrary index = 2), it may be concluded that the conjugate shows high selectivity/affinity to EGFR-expressing cancer cells.

In addition, the cytotoxicities of TPL and Cet-TPL were also examined on normal human bronchial epithelium cell line, BEAS-2B, and human lung fibroblast cell line, MRC-5. TPL also significantly inhibited *in vitro* proliferation of these two cell lines, and the lung fibroblast MRC-5 cell was more resistant to TPL, whereas Cet-TPL effectively suppressed the proliferation of BEAS-2B cells that highly express EGFR, but rarely affected the proliferation of MRC5 in which EGFR is undetectable (Figure S2), further indicating that Cet-TPL specifically targets all cells that highly express EGFR.

In Vivo Suppression of Cet-TPL on EGFR-Overexpressing Cancer Growth

We further investigated the specific antitumor efficacy of Cet-TPL on xenografts of EGFR-expressing A549 cancer cells and two patient-derived xenografts (PDX1 and PDX2) derived from two lung adenocarcinoma individuals in non-obese diabetic (NOD)/severe combined immunodeficiency (SCID)/interleukin-2 receptor (IL-2R) gamma null mice (NSG) mice. The data of tumor volume of subcutaneous xenografts show that, compared with the groups treated with Cet or TPL alone, only Cet-TPL significantly suppressed the *in vivo* growth of NSCLC A549 and PDX1 xenografts (Figure 3A). Although PDX2 and UM-SCC6 were sensitive to Cet and TPL, compared with Cet or TPL alone, Cet-TPL (50 mg/kg) still displayed a significantly stronger inhibition on the *in vivo* growth of these two xenografts (Figure 3A). Consistently, the weights of cancer xenografts treated with Cet-TPL were significantly lower than those treated with Cet and TPL alone. We also observed that a lower dose of 25 mg/kg Cet-TPL also significantly suppressed the *in vivo* growth of A549 xenografts and lung cancer PDX1 (Figure S3). The dosage of 0.5 mg/kg TPL did not significantly suppress the growth of A549 xenografts' growth, and then other xenografts were treated with 1.0 mg/kg TPL. In addition, we also tested a combination of free Cet (equal to Cet control) plus TPL (the amount of

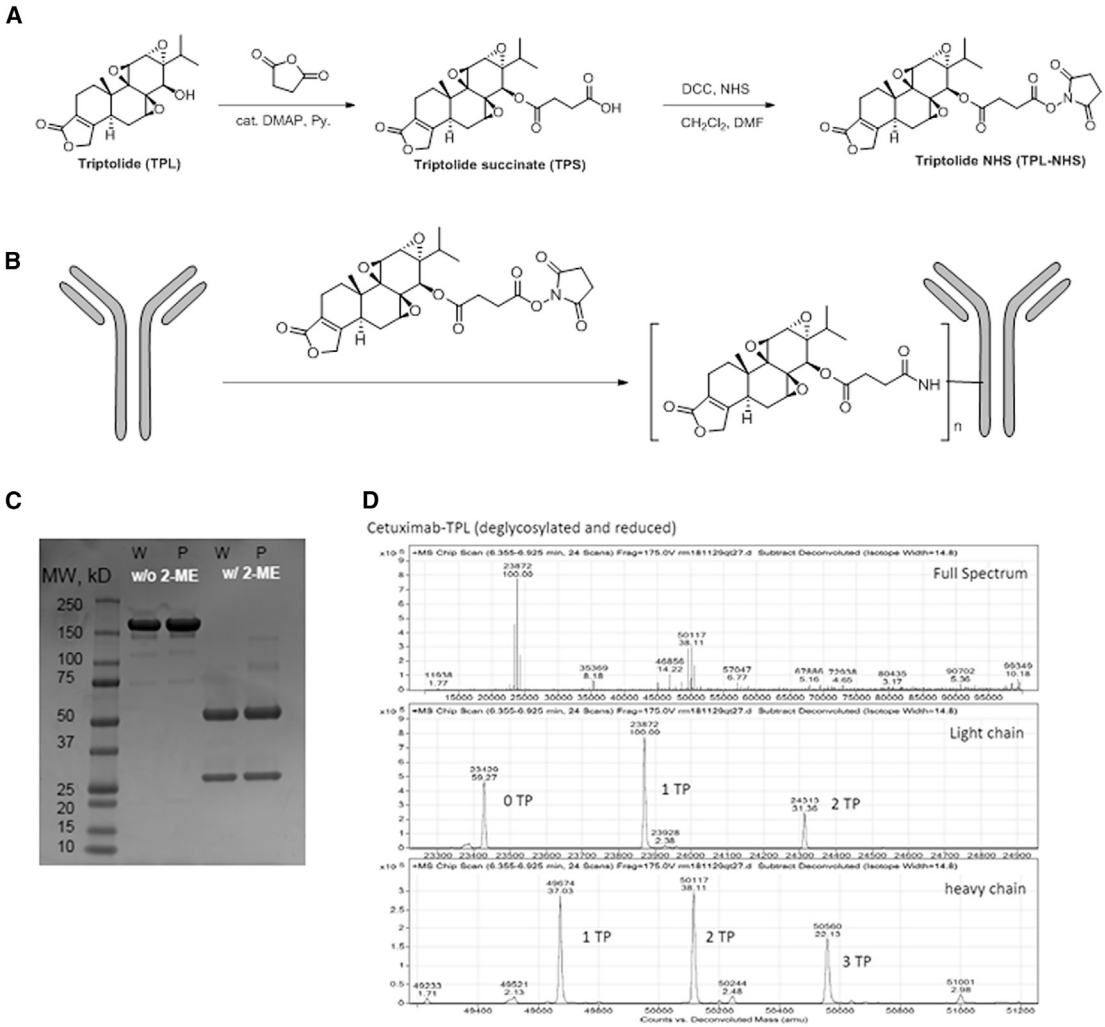

Figure 1. Synthesis and Physical and Chemical Characteristics of Cet-TPL

(A) Schematic of chemical synthesis of triptolide (TPL)-NHS from TPL. (B) Schematic of chemical conjugation of cetuximab (Cet) with TPL-NHS and the formation Cet-TPL conjugate. (C) SDS-PAGE gel for Cet (W), Cet-TPL conjugate (P), loaded with Laemmli sample buffer without (w/o 2-ME) or with 2-mercaptoethanol (w/2-ME) as marked. (D) The mass spectrum of Cet (deglycosylated and reduced) in the full spectrum (upper diagram), for the light chain of the antibody (middle diagram), and for the heavy chain of the antibody (lower diagram). An average of about 5.5 TPLs per Cet was observed. P, Cet-TPL conjugates purified by FPLC; W, Cet.

TPL is close to the amount of conjugated TPL on Cet-TPL) on the *in vivo* growth of A549 xenografts; the outcomes of the experiment indicated that the combination did not significantly suppress the *in vivo* growth of A549 xenografts (Figure S4). Moreover, we also examined whether Cet-TPL nonspecifically suppressed the *in vivo* growth of xenografts generated by H520 that does not express EGFR, and it turned out that Cet-TPL showed no inhibitory effects on the *in vivo* growth of H520. In all, the data of the above experiments clearly demonstrate that Cet-TPL specifically suppresses EGFR-expressing cancer xenografts.

The toxicity of TPL limits its clinical use; Cet-TPL is developed to decrease systemic toxicity of TPL through specifically delivering TPL to cancer cells. Therefore, the adverse effects or toxicity of TPL in mice were recorded and compared with that of Cet-TPL. During the treatment, signs of side effects, such as decreased activity, ruffled fur, decreased appetite, increased stool frequency and diarrhea, weight loss, and death first occurred on the mice administered with TPL, and no abnormal symptoms of toxicity were observed in mice administrated with Cet-TPL and other regimens. It should be noted that the administration of these regimens to tumor-bearing mice did not last longer, because the experiment was terminated as soon as a mouse exhibited the above-abnormal symptoms, especially weight loss and death. Compared with mice given other regimens, the weight of mice administered with TPL was slightly decreased at the end of the experiment (Figure S5), and 4 out of 32 mice died of TPL treatment, whereas no mouse was dead in groups treated with Cet-TPL and other

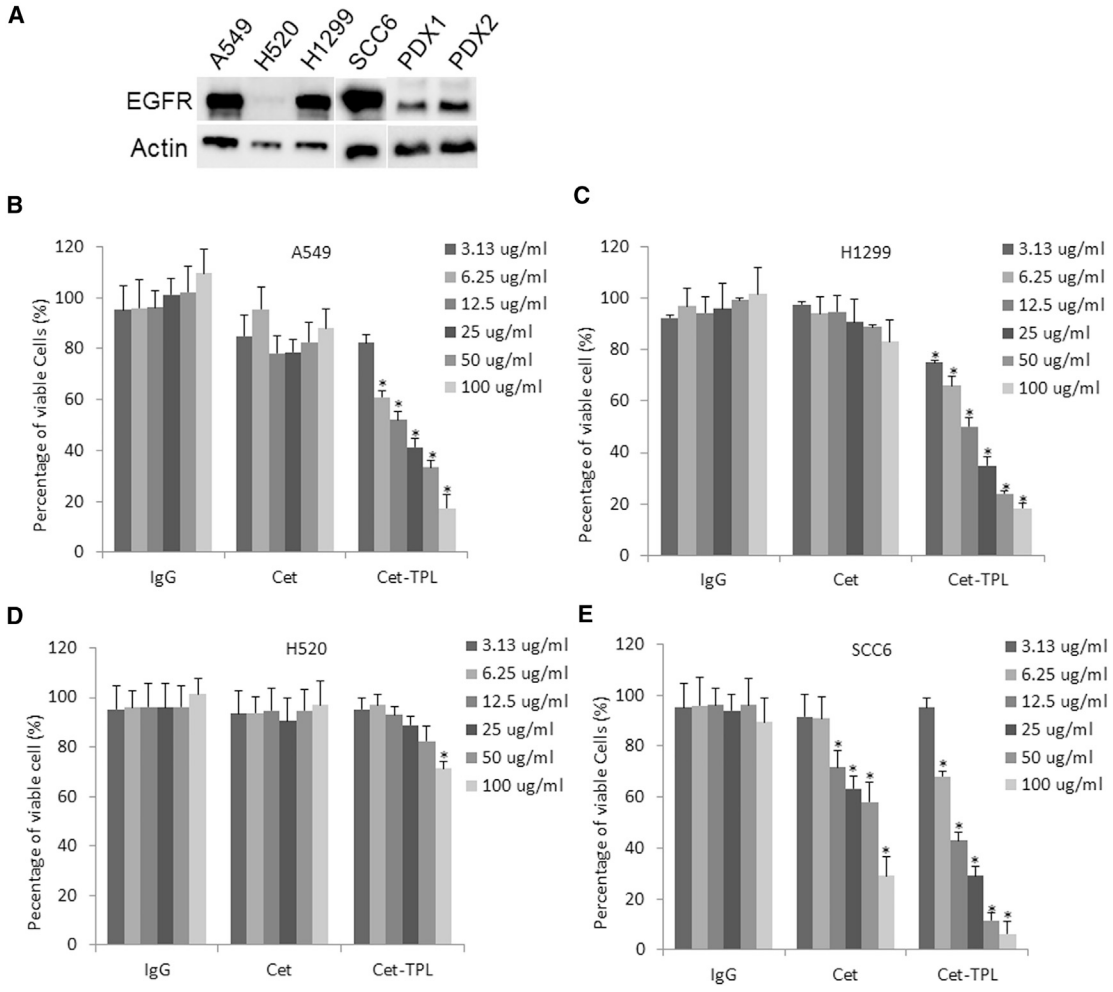

Figure 2. *In Vitro* Cytotoxicity of Cet-TPL to EGFR-Overexpressing Cancer Cells

(A) Western blot analysis of EGFR in NSCLC cell lines A549, H1299, H520, PDX1, and PDX2 of human NSCLC. (B–E) A bar graph depicting the inhibitory effect of IgGs, Cet, and Cet-TPL (conjugate) on *in vitro* cell proliferation for 72 h of (B) A549, (C) H1299, (D) H520 cells, and (E) UM-SCC6 (SCC6). The data are the average of triplicate experiments; *$p < 0.05$ compared with the untreated parent cells.

regimens. Consideration of the amount of TPL showed it was about 2-fold of the calculated amount of conjugated TPL on Cet-TPL conjugate used in the study; therefore, compared with TPL, Cet-TPL has stronger *in vivo* antitumor effects but much less systemic toxicity in mice.

Cet-TPL Significantly Decreased Ki-67-Positive Cancer Cells and Induced More Apoptosis in EGFR-Overexpressing Cancer Xenografts

The Ki-67 protein, a marker used to reflect cellular proliferation, was analyzed in these cancer tissues by immunohistochemistry (IHC) analysis. As shown in Figure 4, compared with the control (vehicle), TPL, and Cet alone, the Cet-TPL dramatically decreased the Ki-67-positive cancer cells in A549 xenografts (Figure 4A) and PDX1 (Figure 4B), whereas it did not decrease Ki-67-positive cancer cells in H520 cells (Figure 4C). Quantitative analysis of Ki-67 IHC stains revealed, compared with these tissues treated with other regimens, the percentage of Ki-67-positive cancer cells was drastically decreased in EGFR-expressing xenograft tissues treated with Cet-TPL (Figure 4D), which was consistent with the *in vitro* data of cytotoxic assays, indicating the *in vivo* growth of EGFR-expressing cancers was specifically significantly inhibited by the Cet-TPL. Because compared with other cancer cells A549 cancer cells are less sensitive to both Cet and TPL, we compared the apoptosis induced by these treatments in A549 xenografts via staining and qualifying the cleaved caspase-3 protein, and the analysis shows that Cet-TPL induced significantly more apoptosis than Cet and TPL alone (Figure 4E), and quantitative analysis showed that the percentage of cleaved caspase-3-positive cancer cells was much higher in A549 xenograft tissues treated with Cet-TPL than others (Figure 4F), indicating Cet-TPL treatment induced significant *in vivo* apoptosis in A549 xenografts.

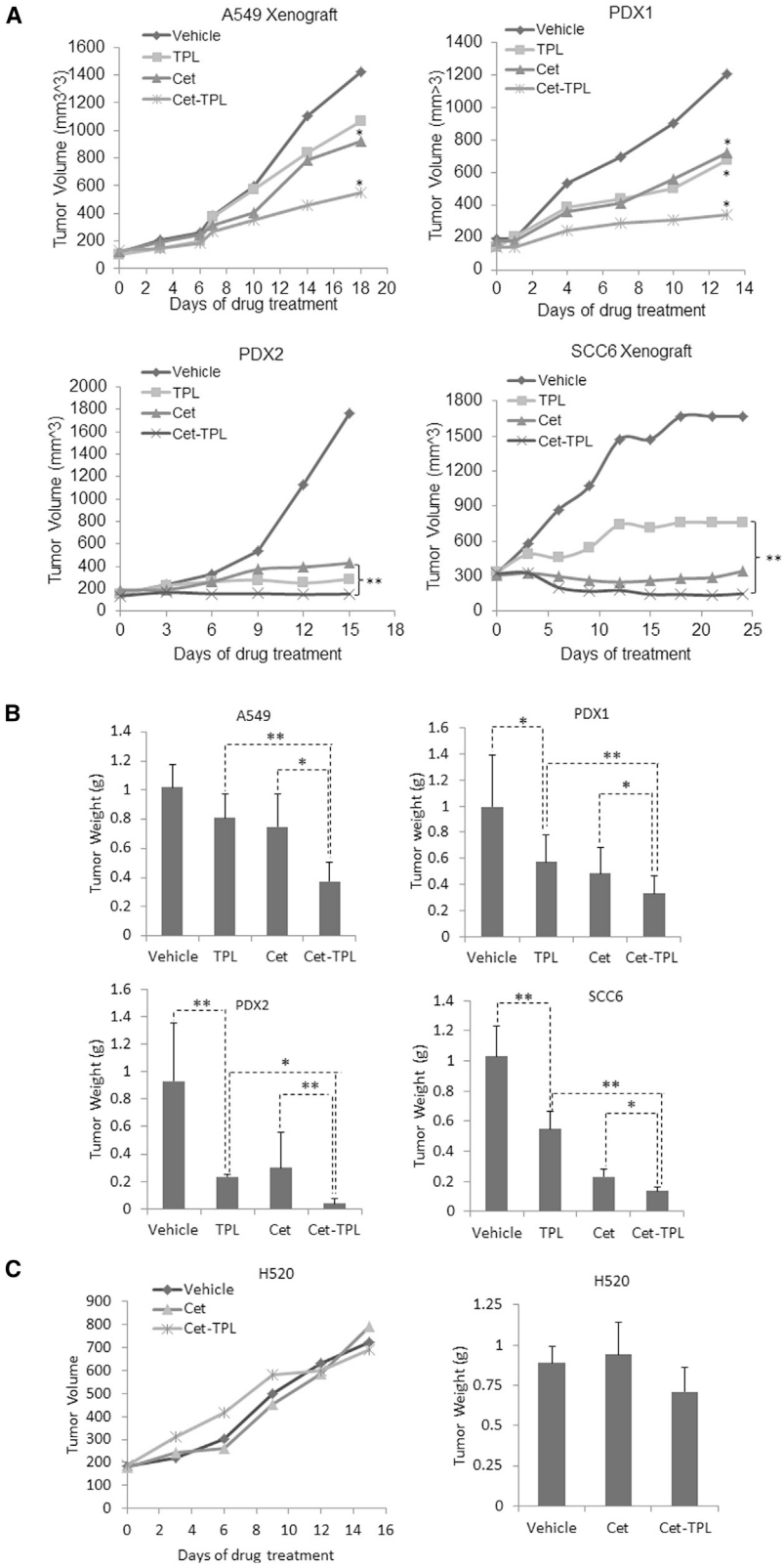

Figure 3. Treatment of EGFR-Overexpressing Cancer Xenografts with Cet-TPL Significantly Suppressed *In Vivo* Tumor Growth

(A) A line graph depicting the growth curves of A549, PDX1, PDX2, and UM-SCC6 (SCC6) xenografts treated with vehicle (IgG), TPL, Cet, or Cet-TPL (conjugate). Data are presented as mean ± SD of eight mice (*$p < 0.05$, compared with vehicle). (B) Bar graphs of the weights of A549, PDX1, PDX2, and SCC6 xenografts in mice treated with Cet (50 mg/kg), TPL (0.5 mg/kg for A549 xenografts and 1 mg/kg for others), or Cet-TPL (50 mg/kg); data are presented as mean ± SD; *$p < 0.05$, **$p < 0.01$, as compared with vehicle/TPL. (C) The *in vivo* growth curves (left panel) and weights of H520 xenografts (right panel) treated with vehicle, Cet (50 mg/kg), and Cet-TPL (50 mg/kg).

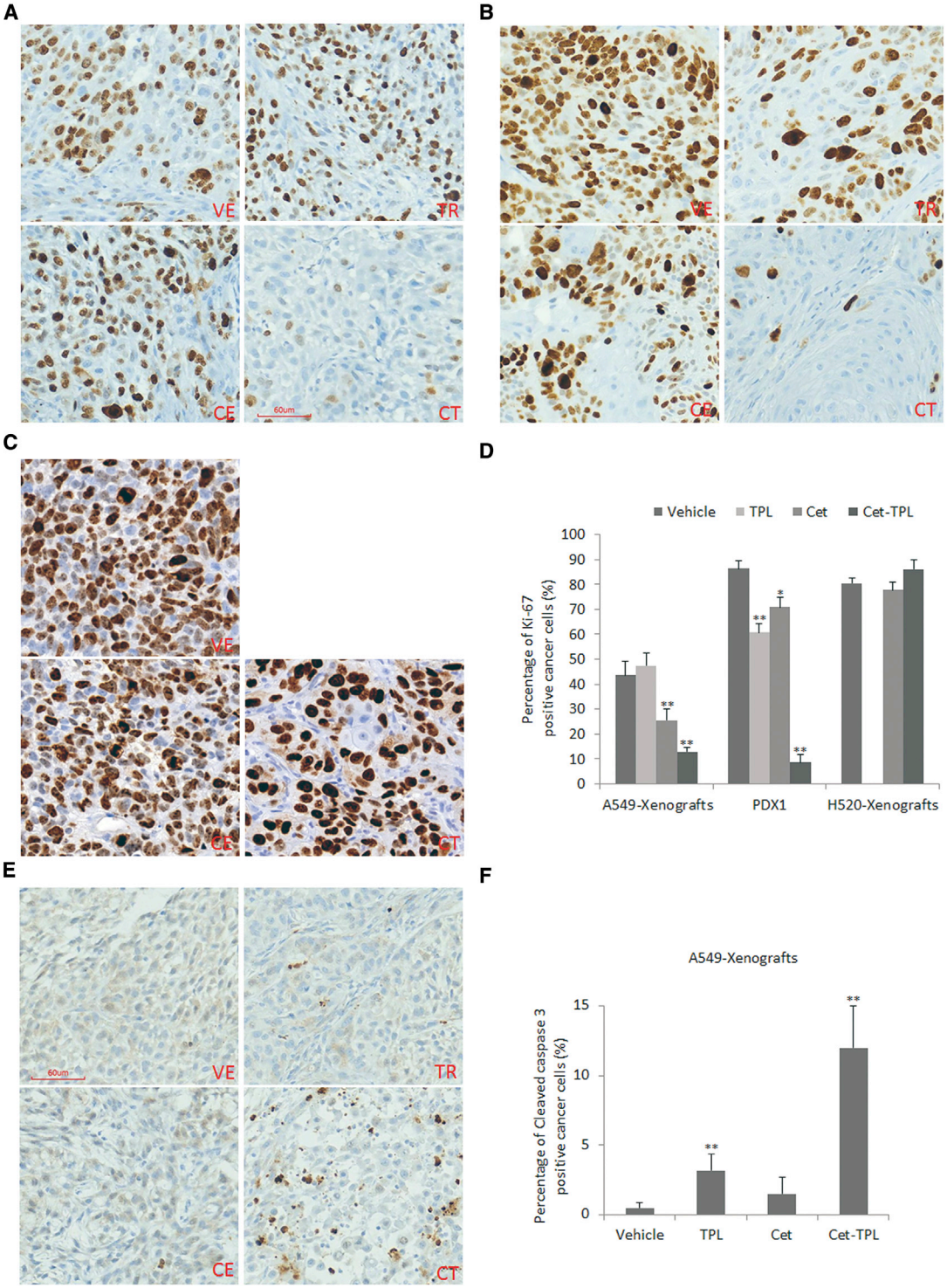

Figure 4. Immunohistochemistry Analysis of Proliferation Marker Ki-67 in Cancer Xenografts Treated with Cet-TPL

(A–C) Ki-67 staining in (A) A549 xenografts, (B) PDX1, (C) H520 xenografts treated with vehicle (VE), TPL (TR), Cet (CE), and Cet-TPL conjugate (CT). (D) Quantitative analysis of the percentage of Ki-67-positive cancer cells in these xenograft tissues. (E) Apoptotic marker cleaved caspase-3 IHC staining in A549 xenografts treated with Cet-TPL. (F) Quantitative analysis of the percentage of cleaved caspase 3-positive cancer cells in A549 xenograft tissues treated with Cet-TPL and others. Original magnification: ×200; red bar: 60 μm.*$p < 0.05$, **$p < 0.01$, compared with vehicle.

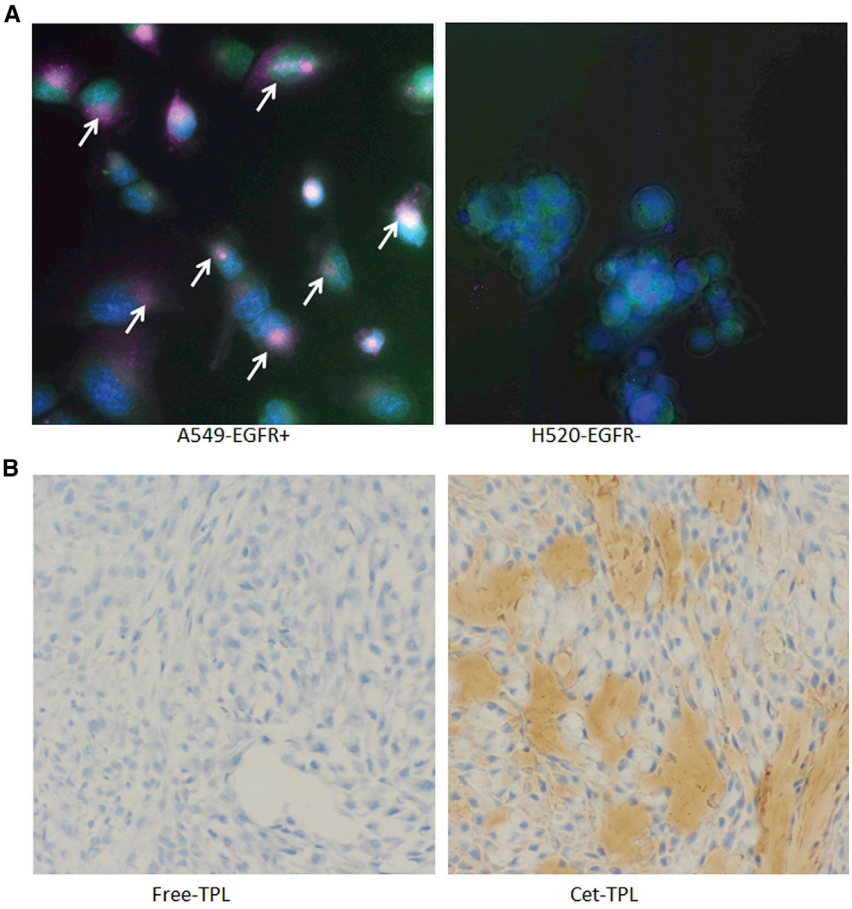

Figure 5. Internalization and Distribution of Cet-TPL in EGFR-Expressing Cancer Cells and Xenografts

(A) Immunofluorescence of an Alexa red fluorescein (red)-labeled Cet-TPL conjugate with LysoTracker Green (green) to localize Cet-TPL and lysosome in A549 cells (left panel) and H520 cells (right panel); the arrows show the colocalization of red (Cet-TPL) and green (lysosome) stains in A549 cells. (B) The *in vivo* distribution of Cet-TPL in A549 xenograft tissues stained by HRP-labeled anti-human IgG. Left panel: xenograft treated with TPL; right panel: xenograft treated with Cet-TPL.

Internalization and Distribution of Cet-TPL in Cancer Cells and Xenografts

We then explored the mechanism of action of Cet-TPL by first confirming its binding and internalization in EGFR-expressing cancer cells. As expected, Cet-TPL binds to its target EGFR to form a Cet-TPL-EGFR complex, leading to endocytosis of the complex. The internalized complex undergoes lysosomal processing, and the cytotoxic TPL is released inside of cells. The released free TPL binds to its target, leading to cell death. We first examined whether Cet-TPL normally bound to EGFR on the surface of cancer cells and then was efficiently internalized. Using an Alexa red fluorescein (red)-labeled Cet-TPL with LysoTracker Green (green) to show lysosome in living cells, we tracked the binding and internalization of Cet-TPL in EGFR-expressing A549 and EGFR-negative H520 cells after it was incubated with cells for 6 h and then was washed off. Immunofluorescence analysis showed that the red fluorescence of Cet-TPL can be detected on both cell membrane and cytoplasm, and colocalized with LysoTracker Green in EGFR-expressing A549 cells (Figure 5A, left panel), whereas the red fluorescence of Cet-TPL was not observed either on the membrane or in the cytoplasm of EGFR-negative H520 cells (Figure 5A, right panel), indicating that Cet-TPL can specifically bind to the surface of EGFR-expressing cancer cells and then internalize and transport to lysosome. In addition, we also tracked the *in vivo* distribution of Cet-TPL in A549 xenografts by staining tissues with horseradish peroxidase (HRP)-labeled anti-human IgG. IHC analysis shows that Cet-TPL (brown staining) was indeed accumulated in the xenograft tissues (Figure 5B). Therefore, the above data indicate that Cet-TPL can be delivered and specifically internalized and processed by EGFR-expressing cancer cells.

Cet-TPL Efficiently Suppresses Pol II and Induced Apoptosis in Cancer Cells

It was reported that Pol II is a target that dominantly mediates the biological activity of TPL.[13] Therefore, we examined the impact of Cet-TPL on Pol II in comparison with that of TPL. After cancer cells were incubated with free TPL for 6 h, a dosage-dependent decrease of both total and phosphorylated RNA polymerase II largest subunit (RPB1, herein Pol II) was induced in both A549 (Figure 6A, left panel) and H1299 (Figure 6B, left panel) cancer cells; at this time point a decrease of these two proteins was not observed in these cancer cells incubated with Cet-TPL (data no shown), while at 18 h post-incubation, a dosage-dependent dramatic decrease of both total and phosphorylated Pol II was observed in both A549 (Figure 6A, right panel) and H1299 (Figure 6B, right panel) cancer cells, indicating that similar to the free TPL, Cet-TPL can efficiently target Pol II of cancer cells *in vitro*.

Cet-TPL Efficiently Induces Apoptosis in Cancer Cells

In addition, we also compared apoptosis induced by free TPL and Cet-TPL. Treatment of TPL can promptly induce apoptosis that was displayed by cleaved PARP protein in both A549 (Figure 7A) and H1299 (Figure 7B) cells at a dosage-dependent manner as early as cancer cells were incubated with TPL for about 6 h. Although the apoptosis induced by Cet-TPL was delayed in comparison with that of TPL, and pronounced apoptosis induced by Cet-TPL was observed in A549 (Figure 7C) and H1299 cells (Figure 7D) after the cancer cells were incubated with Cet-TPL for 18 h, indicating the time course of induced apoptosis was consistent with that of inhibition and degradation of Pol II.

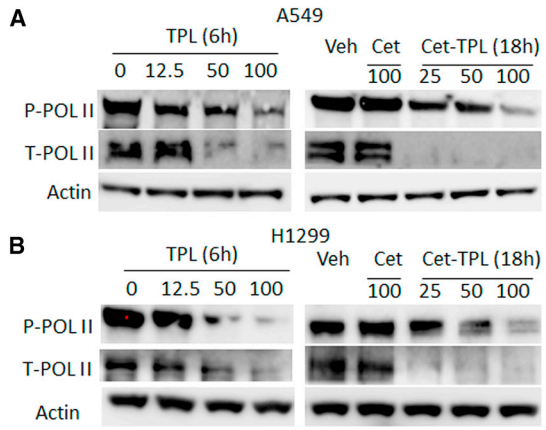

Figure 6. Suppression of Cet-TPL on RNA Polymerase II in Cancer Cells
(A and B) Western blot analysis of the total and phosphorylated Pol II in (A) A549 and (B) H1299 cancer cells treated with TPL (nM) for 6 h (left panels) and Cet-TPL (μg/mL) for 18 h, respectively.

Cet-TPL Efficiently Suppresses Multiple Histone H3 Lysine Methylations and EGFR Signaling Pathways in Cancer Cells

We previously found that TPL modified global epigenetic changes of histone H3 that were also associated with induced apoptosis in lung cancer cells.[16] Therefore, we also examined the inhibitory efficacy of TPL and Cet-TPL on global epigenetic change in multiple histone H3 lysine dimethylations in NSCLC cell lines. As shown in Figure 8, after being treated with Cet-TPL for 18 h, global demethylations of H3K4, H3K9, H3K27, H3K36, and H3K79 were dramatically suppressed by Cet-TPL in a dosage-dependent manner in both A549 (Figure 8A) and H1299 cells (Figure 8B), which suggests that suppression on these modifications of H3 may also contribute to the apoptosis induced by Cet-TPL in cancer cells.

Lastly, we also examined the effect of Cet-TPL on EGFR activation of UM-SCC6 xenografts in which the EGFR signaling pathway may play an important role in carcinogenesis and growth. As shown in Figure 8C, like Cet, Cet-TPL efficiently decreased phosphorylated EGFR in xenograft tissues, indicating that Cet-TPL may function as a bi-functional agent that can target Pol II and EGFR signaling pathways in these cancers with an activated EGFR signaling pathway.

DISCUSSION

In this study, we have demonstrated that Cet-TPL, a novel ADC drug that is built by conjugating TPL to the humanized anti-EGFR mAb Cet (Cet-TPL), can specifically deliver TPL to EGFR-overexpressing cancer cells and verified the *in vivo*-specific and potent antitumor efficacy of Cet-TPL in lung cancer and head and neck cancer models. We believe this agent is likely to also be effective in a variety of other EGFR-expressing cancers.

TPL has been shown to inhibit cell growth and lead to cell death in many cancer cell lines at low dosages. The major obstacles for TPL to becoming a clinically useful drug include its general toxicity at high dosage and lack of water solubility.[19,20] ADCs were initially developed to selectively deliver cytotoxic agents to cancer cells through specific binding of an antibody to cancer-selective targets.[29,30] So far, three ADCs, gemtuzumab ozogamicin, brentuximab vedotin, and inotuzumab ozogamicin, have been approved for hematologic cancers, and one ADC, trastuzumab emtansine, has been approved to treat breast cancer; approximately 80 ADCs are in clinical development in nearly 600 clinical trials, and 2–3 novel ADCs are likely to be approved within the next few years.[29] Two ADCs inhibiting topoisomerase I activity, trastuzumab deruxtecan targeting HER2 in breast and gastric cancers and sacituzumab govitecan targeting Trop2 in breast and lung cancers, are being examined in clinic.[31]

The EGFR is a member of the ErbB family of cell surface tyrosine kinases that regulate both cell proliferation and apoptosis via signal transduction pathways.[32,33] Overexpression of the EGFR gene has been identified in between 40% and 89% of NSCLCs.[23] EGFR is also overexpressed in approximately 75% of head and neck cancers,[24] 75% of malignant gliomas,[25] and 70% of colorectal cancers,[26] and is overexpressed in a number of other cancers, including renal cell, bladder, and pancreatic cancer.[27] The overexpression of EGFR has been exploited to target tumor cells selectively by small molecular inhibitor and anti-EGFR antibody to block the downstream signaling pathway in some cancers, including colon and head and neck cancers. Cet, a recombinant chimeric monoclonal IgG1 antibody as a EGFR inhibitor, is approved for the first-line treatment in combination with chemotherapy or as a single agent in patients who have failed or are intolerant to chemotherapy with EGFR-expressing, *RAS* wild-type metastatic colorectal cancer.[28,34,35] ADCs targeting EGFR have also been reported to target EGFR-expressing cancers recently.[36,37] In this study, we used Cet, an approved anti-EGFR antibody, as a vehicle to specifically deliver TPL to EGFR-expressing lung cancers and others.

It is well-known that an efficient ADC requires optimization of multiple parameters, including antigens, antibodies, linkers, payloads, and the payload-linker linkage.[38,39] In general, interchain disulfide bridges and surface-exposed lysines are the most currently used residues on the antibody for conjugation to cytotoxic payloads.[40] Theoretically, the linkage of cytotoxic payloads to the surface-exposed lysine of mAbs occurs after conjugation of ~40 lysine residues on both heavy and light chain of mAbs, and it results in 0–8 cytotoxic payload linkages per antibody and heterogeneity with about one million different ADC species.[38–40] By controlling the ratio of TPL-NHS to antibody, we got Cet-TPL with various drug-to-antibody ratios (DARs) of 0.4, 2, 4, and 6 (calculated based on mass spectrum results; data not shown). We first characterized and optimized the DAR of Cet-TPL and examined the efficacy of Cet-TPL with various DARs. We found that DAR <2 did not work as efficiently as these conjugates with a DAR from 4 to 6 (Figure S6), so we optimized our synthesis of Cet-TPL with DARs of 4–6, and the average of DAR is about 5 for the following study. We did not increase the DAR further because of a study suggesting that antibody conjugates with a DAR ranging from 2 to 6 have a better therapeutic index, less liver accumulation,

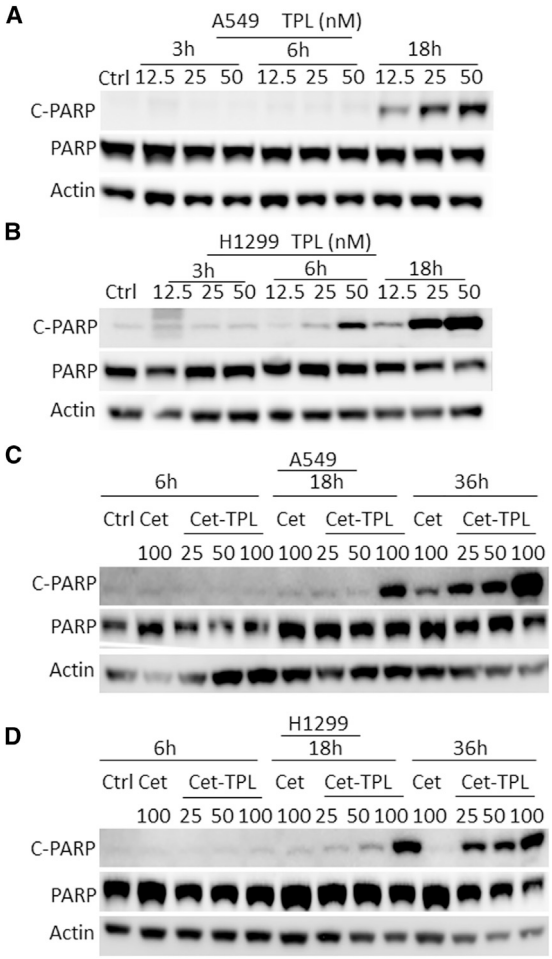

Figure 7. Induced Apoptosis by Cet-TPL in Cancer Cells

(A and B) Western blot analysis of the apoptosis marker: cleaved PARP protein in both (A) A549 and (B) H1299 treated with a given concentration of TPL (nM) for 3, 6, and 18 h. (C and D) Western blot analysis of the cleaved PARP protein in both (C) A549 and (D) H1299 treated with a given concentration of Cet-TPL (μg/mL) for 6, 18, and 36 h.

and less clearance rates than these conjugates with a very high DAR (~9–10).[41] Binding and internalization, circulating stability, and penetration of ADC are also essential to its cytotoxic effect of Cet-TPL. In the study, we also clearly demonstrated that the conjugation does not impact Cet's binding affinity, and the Cet-TPL conjugate can be effectively internalized in EGFR-expressing cancer cells. Also, biodistribution studies in xenograft tissues showed that the conjugate could penetrate to the tumor microenvironment of subcutaneous xenografts after intraperitoneal injection. Therefore, these data of *in vitro* and *in vivo* experiments have convincingly indicated that Cet-TPL can efficiently deliver TPL and transfer it into cancer cells.

TPL has been shown to have potent antiproliferative and cytotoxic activities, and it is also effective against cancer in animal models.[10,14,42] TPL and derivatives have entered human clinical trials for cancer treatment.[21] We also have shown that treatment with TPL and its derivative leads to decreased lung cancer cell proliferation, invasion, and metastasis of lung cancer.[16–18] At the cellular level, TPL shows strong antiproliferative activity, inhibiting the proliferation of all 60 US National Cancer Institute cancer cell lines with IC_{50} values in the low nanomolar range (average IC_{50} = 12 nM).[13] In this study, we also examined its effect on several lung cancer cells and found the IC_{50} of TPL to some cancer cells is as low as 6.25 nM. At the molecular level, TPL was shown to perturb multiple signaling pathways, including NF-κB,[9] HSP70,[10] BCL-2,[11] and p53 pathways.[12] In all, TPL is a potential and ideal cytotoxic agent for cancer therapy.

The inhibition of Pol II-mediated transcription via TPL covalently binding to and blocking its DNA-dependent ATPase activity XPB, a subunit of the transcription factor TFIIH, has been confirmed to account for the majority of the known biological activities of TPL.[13] Therefore, it is supposed that Cet-TPL conjugates would enter cancer cells through EGFR, whereby the linker would undergo cleavage to release TPL, allowing it to bind to XPB and block cell proliferation or induce apoptosis. In agreement with this, we here have also demonstrated, similar to TPL, that Cet-TPL effectively decreased both total and phosphorylated Pol II, as well as the multiple lysine dimethylation of histone H3, and induced apoptosis in the EGFR-positive cancer cells in a dosage-dependent manner.[13,16] Notably, Cet-TPL showed significant cytotoxicity against EGFR-positive cell lines, but not EGFR-negative counterparts, in a dose-dependent manner. Moreover, we showed that Cet-TPL significantly suppresses the *in vivo* growth of EGFR-expressing cancer cells. Compared with TPL, the effects of Cet-TPL were delayed but selective. The *in vivo* growth of xenografts generated by A549 lung cancer cells and PDX1 that are resistant to Cet and TPL were significantly suppressed by Cet-TPL, whereas the *in vivo* growth of xenografts generated by UM-SCC6 and PDX2 that were sensitive to both Cet and TPL were also significantly suppressed by Cet-TPL compared with Cet or TPL alone. In addition, Cet-TPL also efficiently suppresses the activated EGFR pathway in UM-SCC6 cancer cells. TPL is toxic at higher doses and has relatively poor pharmacokinetics, and the lethal dose (LD_{50}) of TPL was reported as <1 mg/kg body weight in mice.[43] We also observed a severe toxicity of TPL, although we did not observe any significant toxicities (the most common being slight weight loss, decreased appetite, and increased stool frequency and diarrhea) in the mouse models treated with Cet-TPL. We envision that conjugating TPL with Cet could also increase its selectivity for tumor cells, thereby decreasing its toxicity. Compared with the *in vitro* IC_{50} to lung cancer cells, the efficacy of Cet-TPL may be 1/50 of free TPL, and we speculate that the low *in vitro* efficiency may be partially caused by the delayed time course of cells' response to Cet-TPL, and an extended incubation of Cet-TPL with cancer cells may kill more cancer cells and then further decrease the *in vitro* IC_{50} of Cet-TPL. Of interest, compared with free TPL, the Cet-TPL has a better *in vivo* anticancer effect. We believe the conjugate may change the stability and distribution of TPL, because the IgG portion of the ADC is important for maintaining a long half-life, binding to target, and internalizing drug into tumor cells, and the longer half-life of the

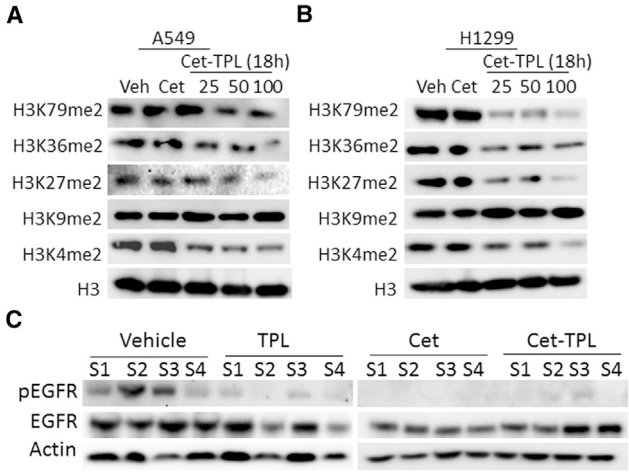

Figure 8. Suppression of Cet-TPL on Multiple Histone H3 Lysine Methylations and EGFR Signaling Pathways in Cancer Cells

(A and B) Western blot analysis of global demethylation of H3K4, H3K9, H3K27, H3K36, and H3K79 in (A) A549 and (B) H1299 cells treated with Cet-TPL (μg/mL) for 18 h. (C) Western blot analysis of phosphorylated EGFR in xenografts of UM-SCC6 treated with vehicle, TPL, Cet, and Cet-TPL (conjugate); S1–S4 for four individual samples. Veh, vehicle.

IgG allows for greater absolute drug accumulation into tumors over time.[44] In all, compared with TPL, Cet, or their combination, Cet-TPL displays higher target-specific cytotoxicity against EGFR-expressing cancers and much lower *in vivo* systemic toxicity.

Taken together, the present study provides convincing evidences that Cet-TPL can effectively bind to EGFR and then is internalized inside of cancer cells; finally it releases TPL to suppress Pol II in EGFR-expressing cancer cells, resulting in growth suppression of cancer cells. We have verified that the novel Cet-TPL showed strong antitumor properties against EGFR-positive cancers both *in vitro* and *in vivo* without severe toxicity. Therefore, Cet-TPL represents a potent targeting therapeutic agent against EGFR-overexpressing NSCLC and other cancers.

MATERIALS AND METHODS

Synthesis and Characterization of Cet-TPL Conjugate

Schematic of chemical conjugation of Cet with TPL is shown in Figures 1A and 1B. After succinic anhydride (1,200 mg, 12 mM) and 4-dimethylaminopyridine (DMAP) (72 mg, 0.6 mM) were added to a solution of TPL (1,080 mg, 3 mM) in pyridine (6 mL), the mixture was stirred overnight and diluted with ethyl acetate, then washed with saturated copper sulfate, water, and brine, respectively. The organic layers were dried over Na_2SO_4 and filtered. The filtrate was concentrated and purified by silica gel column chromatography (CH_2Cl_2/CH_3OH, 15:1) to give the compound TPL succinate (TPS) (1,100 mg, 2.4 mM, 80%) as a white solid powder.[45]

TPS (200 mg, 0.44 mM) in dimethylformamide (DMF) (0.5 mL) and dichloromethane (4 mL) was added to *N,N′*-dicyclohexylcarbodiimide (DCC) (108 mg, 0.52 mM) and *N*-hydroxysuccinimide (NHS) (56 mg, 0.49 mM). After stirring overnight, the mixture was filtered and concentrated under a vacuum. The residue was purified by silica gel column chromatography (CH_2Cl_2/EtOAc, 3:1) to give TPL-NHS (170 mg, 0.3 mM, 70%) as a white solid powder.

Cet (2 mg/mL) in 550 mL phosphate-buffered saline (PBS) in a 1,000-mL glass bottle was added to TPL-NHS (80 mg, 20 eq.) in 8 mL *N*, *N*-dimethylacetamide. The solution was gently stirred at room temperature for 1 h. Tris buffer (1M [pH 8.0], 150 mL) was added to quench the reaction and stirred for 30 min. Solution was concentrated by centrifugal filters (Amicon Ultra-15) and purified by size-exclusion chromatography (HiLoad 26/600 Superdex 200). Concentrations of the products were measured using A280. Purities were checked by SDS-PAGE gels with or without reducing reagent 2-ME as indicated. Cet control or purified Cet-TPL conjugates were treated with Rapid PNGase F kit (New England Biolabs) to remove the N-linked glycans and to reduce the antibody to light chain and heavy chain before injecting on a quadrupole time-of-flight (Q-TOF) mass spectrometry for easier observation. DARs were calculated by the relative abundance of each individual peak from mass spectrum results.

Cell Culture and Cytotoxicity Assay

Human lung cancer cell lines, A549 (p53 wild-type, K-Ras mutated), H1299 (p53 null, N-Ras mutated), and H520 (p53 mutated), head and neck squamous carcinoma cell line UM-SCC-6 (SCC6) cells, and human normal fibroblast cell line MRC5 (CCL-171) were purchased from American Type Culture Collection (ATCC). BEAS-2B (CRL-9609; ATCC) immortalized human bronchial epithelial cell line was derived from normal bronchial cells by immortalization with an adenovirus 12-SV-40 hybrid virus, and it was cultured in serum-free growth factor-supplemented BEBM™ (bronchial epithelial cell growth basal medium, Lonza), as described previously.[46] All other cells were cultured in DMEM, Eagle's minimal essential medium (EMEM), or RPMI medium supplemented with 10% fetal bovine serum (FBS), 100 U/mL penicillin, and 100 mg/mL streptomycin. The cytotoxic effects of TPL, Cet, and Cet-TPL against cancer cell lines were measured using the colorimetric cell proliferation cell counting kit-8 (CCK-8). For proliferation assay, cells were seeded in 96-well plates in four to six replicates at densities of 2.0×10^3 cells per well; after 24 h, 3.125–100 μg/mL IgG, Cet, and Cet-TPL were added to wells, respectively, and further incubated with cells for 72 h. Then 10 μL CCK-8 solution was added to each well and further developed for 2 h. The absorbance values were detected at a wavelength of 450 nm using a Bio-Rad microplate reader. The cell viability was calculated by the optical density (OD) values of treated groups/OD values of control groups (vehicle/PBS) × 100%. IgG also serves as a control for Cet, and cell proliferation was monitored at 72 h using CCK-8. The IC_{50} of TPL and Cet-TPL to each cell was also calculated accordingly.

Xeno-transplantation and Treatment of Xenografts with Cet, TPL, and Cet-TPL

This study was reviewed and approved by the Institutional Review Board (IRB; #12299) of City of Hope National Medical Center. All

animal protocols were performed in the animal facility at City of Hope National Medical Center in accordance with federal, local, and institutional guidelines. All experiments using human material were performed in accordance with all relevant guidelines and regulations, and informed consent had been obtained from donors. NSG mice (24–27 g, 6–8 weeks of age; Jackson Labs, Bar Harbor, ME, USA) were used for xenograft experiment. Freshly harvested tumor specimens from primary lung adenocarcinoma patients who underwent surgical resection with curative intent without preoperative chemoradiotherapy were subcutaneously implanted in NSG mice to generate PDX. When subcutaneous xenograft tumors reached ~1.5 cm^3, they were serially passaged in NSG mice by subcutaneous transplant (0.10–0.12 g, 2 × 2 mm) under general anesthesia.[47] In the study, two PDXs originating from two primary lung adenocarcinoma individuals were used to examine the *in vivo* anticancer efficacy of the conjugate. To establish xenografts of cancer cell lines, a suspension of 5×10^6 H1299, UM-SCC6 cancer cells in 0.1 mL RPMI 1640 was injected into the subcutaneous dorsa of mice at the proximal midline. When the tumor volume was about 90–110 mm^3, mice were randomized into five or six treatment groups, and each group included seven to eight mice. Also, mouse treatment was performed by intraperitoneal injection of vehicle (PBS), 0.5 or 1.0 mg/kg TPL, 50 mg/kg Cet, and 25 and 50 mg/kg Cet-TPL in <300 μL PBS twice/week for about 2–3 weeks. The weight of the mice was recorded, and tumor volumes were measured and calculated (0.5 × [long dimension] × [short dimension]^2) two to three times weekly. All animals were euthanized before tumors reached 3,000 mm^3 or showed signs of reduced appetize, weight loss, or impending ulceration. At the end of the experiment, mice were euthanized and xenograft tissues were removed and weighted. Data are presented as average ± SD (*$p < 0.05$, compared with vehicle controls).

Western Blot, IHC, and Immunofluorescence

The antibodies against Actin (catalog number [Cat#]: SC-47778), total Pol II (Cat#: SC-55492), and phosphorylated Pol II (Cat#: SC-47701) for western blot analysis were purchased from Santa Cruz Biotechnology. The antibody against poly (ADP-ribose) polymerase (PARP; Cat#: PA5-77850) was purchased from Invitrogen. The antibodies against total EGFR (Cat#: 4267S) and phosphorylated EGFR (Cat#: 2234S), histone 3 (Cat#: 4499S), demethylation of H3K4 (HeK4me2, Cat#: 9725S), H3K9me2 (Cat#: 4658S), H3K27me2 (Cat#: 9728P), and H3K36me2 (Cat#: 2901S) were purchased from Cell Signaling Technology.

A small proportion from each xenograft or PDX tissue was fixed with 4% formalin for 24 h and embedded in paraffin for subsequent histology study. IHC analysis was applied to analyze the proliferation and apoptosis marker proteins in A549 xenograft and PDX tissues using anti-Ki-67 mAb (Cat#: M7240; Dako) and anti-cleave caspase-3 antibody (Cat#: NB100-56113; Novusbio). For quantitative analysis of IHC staining, four regions of each slide were selected randomly; the positively stained cancer cells were counted, and the percentage of positively stained cancer cells to total cancer cells was calculated as described previously.[48,49] Data were presented as the average of percentages of three to four slides.

Cet-TPL was labeled Alexa red fluorescein (red), and the labeled Cet-TPL and LysoTracker Green (green) to show lysosome in living cells were used to track the binding and internalization of Cet-TPL in cancer cells by immunofluorescence analysis as previously reported.[50] In brief, Alexa red fluorescein-labeled Cet-TPL (1 μg/mL) was incubated with cells in culture medium for 2 h, and then cells were washed with PBS; after culturing for an additional 4 h, 100 nM LysoTracker Green DND-26 (Cat#: 8783S; Cell Signaling) was added, and cells with fluorescent staining of Alexa red and DND-26 green were imaged by fluorescence microscope for 5–10 min.

Statistical Analysis

All experiments were performed in duplicates or triplicates and repeated at least two times in each experiment. Two group comparisons were analyzed for variation and significance using a Student's t test or Pearson χ^2 test. All data shown are mean ± SD. Statistical significance was set at $p < 0.05$.

SUPPLEMENTAL INFORMATION

Supplemental Information can be found online at https://doi.org/10.1016/j.omto.2020.07.001.

AUTHOR CONTRIBUTIONS

D.J.R. and D.H. conceived the study and revised the manuscript. K.Z. and Y.M. designed and characterized the conjugate, analyzed and interpreted data, and wrote and revised the manuscript. K.Z., Y.M., and T.S. performed synthesis, cytotoxic assay, and western blot. Y.G. and J.W. did xenograft experiments. R.P.P., M.L., and W.L. provided technical and material support. All authors read and approved the final version of the manuscript.

CONFLICTS OF INTEREST

D.J.R., D.H., K.Z., and Y.M. have filed a patent based on the present work. The other authors have no conflicts of interest to disclose.

ACKNOWLEDGMENTS

This study is supported by Stop Cancer and NIH grants 5K12CA001727-20 and P30CA33572 through the use of several City of Hope Core Facilities. We acknowledge the generous support of the Baum Family Foundation in support of this research. The authors thank Aimin Li and Michael Lewallen at the pathology core for IHC analysis.

REFERENCES

1. Ferlay, J., Shin, H.R., Bray, F., Forman, D., Mathers, C., and Parkin, D.M. (2010). Estimates of worldwide burden of cancer in 2008: GLOBOCAN 2008. Int. J. Cancer *127*, 2893–2917.

2. Chen, Z., Fillmore, C.M., Hammerman, P.S., Kim, C.F., and Wong, K.K. (2014). Non-small-cell lung cancers: a heterogeneous set of diseases. Nat. Rev. Cancer *14*, 535–546.

3. Morgensztern, D., Campo, M.J., Dahlberg, S.E., Doebele, R.C., Garon, E., Gerber, D.E., Goldberg, S.B., Hammerman, P.S., Heist, R.S., Hensing, T., et al. (2015).

Molecularly targeted therapies in non-small-cell lung cancer annual update 2014. J. Thorac. Oncol. *10* (1 Suppl 1), S1–S63.

4. Siegel, R., Ma, J., Zou, Z., and Jemal, A. (2014). Cancer statistics, 2014. CA Cancer J. Clin. *64*, 9–29.
5. Kupchan, S.M., Court, W.A., Dailey, R.G., Jr., Gilmore, C.J., and Bryan, R.F. (1972). Triptolide and tripdiolide, novel antileukemic diterpenoid triepoxides from Tripterygium wilfordii. J. Am. Chem. Soc. *94*, 7194–7195.
6. Liu, Y., Chen, H.L., and Yang, G. (2010). Extract of Tripterygium wilfordii Hook F protect dopaminergic neurons against lipopolysaccharide-induced inflammatory damage. Am. J. Chin. Med. *38*, 801–814.
7. Li, G., Ren, J., Wang, G., Gu, G., Hu, D., Ren, H., Hong, Z., Wu, X., Liu, S., and Li, J. (2014). T2 enhances in situ level of Foxp3+ regulatory cells and modulates inflammatory cytokines in Crohn's disease. Int. Immunopharmacol. *18*, 244–248.
8. Bao, J., and Dai, S.M. (2011). A Chinese herb Tripterygium wilfordii Hook F in the treatment of rheumatoid arthritis: mechanism, efficacy, and safety. Rheumatol. Int. *31*, 1123–1129.
9. Zheng, L., Jia, J., Dai, H., Wan, L., Liu, J., Hu, L., Zhou, M., Qiu, M., Chen, X., Chang, L., et al. (2017). Triptolide-Assisted Phosphorylation of p53 Suppresses Inflammation-Induced NF-κB Survival Pathways in Cancer Cells. Mol. Cell. Biol. *37*, e00149-17.
10. Phillips, P.A., Dudeja, V., McCarroll, J.A., Borja-Cacho, D., Dawra, R.K., Grizzle, W.E., Vickers, S.M., and Saluja, A.K. (2007). Triptolide induces pancreatic cancer cell death via inhibition of heat shock protein 70. Cancer Res. *67*, 9407–9416.
11. Wan, C.K., Wang, C., Cheung, H.Y., Yang, M., and Fong, W.F. (2006). Triptolide induces Bcl-2 cleavage and mitochondria dependent apoptosis in p53-deficient HL-60 cells. Cancer Lett. *241*, 31–41.
12. Sun, Y.Y., Xiao, L., Wang, D., Ji, Y.C., Yang, Y.P., Ma, R., and Chen, X.H. (2017). Triptolide inhibits viability and induces apoptosis in liver cancer cells through activation of the tumor suppressor gene p53. Int. J. Oncol. *50*, 847–852.
13. Titov, D.V., Gilman, B., He, Q.L., Bhat, S., Low, W.K., Dang, Y., Smeaton, M., Demain, A.L., Miller, P.S., Kugel, J.F., et al. (2011). XPB, a subunit of TFIIH, is a target of the natural product triptolide. Nat. Chem. Biol. *7*, 182–188.
14. Manzo, S.G., Zhou, Z.L., Wang, Y.Q., Marinello, J., He, J.X., Li, Y.C., Ding, J., Capranico, G., and Miao, Z.H. (2012). Natural product triptolide mediates cancer cell death by triggering CDK7-dependent degradation of RNA polymerase II. Cancer Res. *72*, 5363–5373.
15. Xiaowen, H., and Yi, S. (2012). Triptolide sensitizes TRAIL-induced apoptosis in prostate cancer cells via p53-mediated DR5 up-regulation. Mol. Biol. Rep. *39*, 8763–8770.
16. Nardi, I., Reno, T., Yun, X., Sztain, T., Wang, J., Dai, H., Zheng, L., Shen, B., Kim, J., and Raz, D. (2018). Triptolide inhibits Wnt signaling in NSCLC through upregulation of multiple Wnt inhibitory factors via epigenetic modifications to Histone H3. Int. J. Cancer *143*, 2470–2478.
17. Reno, T.A., Kim, J.Y., and Raz, D.J. (2015). Triptolide Inhibits Lung Cancer Cell Migration, Invasion, and Metastasis. Ann. Thorac. Surg. *100*, 1817–1824, discussion 1824–1825.
18. Reno, T.A., Tong, S.W., Wu, J., Fidler, J.M., Nelson, R., Kim, J.Y., and Raz, D.J. (2016). The triptolide derivative MRx102 inhibits Wnt pathway activation and has potent anti-tumor effects in lung cancer. BMC Cancer *16*, 439.
19. Chen, B.J. (2001). Triptolide, a novel immunosuppressive and anti-inflammatory agent purified from a Chinese herb Tripterygium wilfordii Hook F. Leuk. Lymphoma *42*, 253–265.
20. Zhou, Z.L., Yang, Y.X., Ding, J., Li, Y.C., and Miao, Z.H. (2012). Triptolide: structural modifications, structure-activity relationships, bioactivities, clinical development and mechanisms. Nat. Prod. Rep. *29*, 457–475.
21. Chugh, R., Sangwan, V., Patil, S.P., Dudeja, V., Dawra, R.K., Banerjee, S., Schumacher, R.J., Blazar, B.R., Georg, G.I., Vickers, S.M., and Saluja, A.K. (2012). A preclinical evaluation of Minnelide as a therapeutic agent against pancreatic cancer. Sci. Transl. Med. *4*, 156ra139.
22. Carter, B.Z., Mak, D.H., Shi, Y., Fidler, J.M., Chen, R., Ling, X., Plunkett, W., and Andreeff, M. (2012). MRx102, a triptolide derivative, has potent antileukemic activity in vitro and in a murine model of AML. Leukemia *26*, 443–450.
23. Lynch, T.J., Bell, D.W., Sordella, R., Gurubhagavatula, S., Okimoto, R.A., Brannigan, B.W., Harris, P.L., Haserlat, S.M., Supko, J.G., Haluska, F.G., et al. (2004). Activating mutations in the epidermal growth factor receptor underlying responsiveness of non-small-cell lung cancer to gefitinib. N. Engl. J. Med. *350*, 2129–2139.
24. Maiti, G.P., Mondal, P., Mukherjee, N., Ghosh, A., Ghosh, S., Dey, S., Chakrabarty, J., Roy, A., Biswas, J., Roychoudhury, S., and Panda, C.K. (2013). Overexpression of EGFR in head and neck squamous cell carcinoma is associated with inactivation of SH3GL2 and CDC25A genes. PLoS ONE *8*, e63440.
25. Higgins, R.J., Dickinson, P.J., LeCouteur, R.A., Bollen, A.W., Wang, H., Wang, H., Corely, L.J., Moore, L.M., Zang, W., and Fuller, G.N. (2010). Spontaneous canine gliomas: overexpression of EGFR, PDGFRalpha and IGFBP2 demonstrated by tissue microarray immunophenotyping. J. Neurooncol. *98*, 49–55.
26. Cohen, R.B. (2003). Epidermal growth factor receptor as a therapeutic target in colorectal cancer. Clin. Colorectal Cancer *2*, 246–251.
27. Sharma, S.V., Bell, D.W., Settleman, J., and Haber, D.A. (2007). Epidermal growth factor receptor mutations in lung cancer. Nat. Rev. Cancer *7*, 169–181.
28. Baselga, J. (2001). The EGFR as a target for anticancer therapy—focus on cetuximab. Eur. J. Cancer *37* (*Suppl 4*), S16–S22.
29. Coats, S., Williams, M., Kebble, B., Dixit, R., Tseng, L., Yao, N.S., Tice, D.A., and Soria, J.C. (2019). Antibody-Drug Conjugates: Future Directions in Clinical and Translational Strategies to Improve the Therapeutic Index. Clin. Cancer Res. *25*, 5441–5448.
30. Schrama, D., Reisfeld, R.A., and Becker, J.C. (2006). Antibody targeted drugs as cancer therapeutics. Nat. Rev. Drug Discov. *5*, 147–159.
31. King, G.T., Eaton, K.D., Beagle, B.R., Zopf, C.J., Wong, G.Y., Krupka, H.I., Hua, S.Y., Messersmith, W.A., and El-Khoueiry, A.B. (2018). A phase 1, dose-escalation study of PF-06664178, an anti-Trop-2/Aur0101 antibody-drug conjugate in patients with advanced or metastatic solid tumors. Invest. New Drugs *36*, 836–847.
32. Ciardiello, F., De Vita, F., Orditura, M., and Tortora, G. (2004). The role of EGFR inhibitors in nonsmall cell lung cancer. Curr. Opin. Oncol. *16*, 130–135.
33. Tokumo, M., Toyooka, S., Kiura, K., Shigematsu, H., Tomii, K., Aoe, M., Ichimura, K., Tsuda, T., Yano, M., Tsukuda, K., et al. (2005). The relationship between epidermal growth factor receptor mutations and clinicopathologic features in non-small cell lung cancers. Clin. Cancer Res. *11*, 1167–1173.
34. Galizia, G., Lieto, E., De Vita, F., Orditura, M., Castellano, P., Troiani, T., Imperatore, V., and Ciardiello, F. (2007). Cetuximab, a chimeric human mouse anti-epidermal growth factor receptor monoclonal antibody, in the treatment of human colorectal cancer. Oncogene *26*, 3654–3660.
35. Wong, S.F. (2005). Cetuximab: an epidermal growth factor receptor monoclonal antibody for the treatment of colorectal cancer. Clin. Ther. *27*, 684–694.
36. Phillips, A.C., Boghaert, E.R., Vaidya, K.S., Mitten, M.J., Norvell, S., Falls, H.D., DeVries, P.J., Cheng, D., Meulbroek, J.A., Buchanan, F.G., et al. (2016). ABT-414, an Antibody-Drug Conjugate Targeting a Tumor-Selective EGFR Epitope. Mol. Cancer Ther. *15*, 661–669.
37. Hu, X.Y., Wang, R., Jin, J., Liu, X.J., Cui, A.L., Sun, L.Q., Li, Y.P., Li, Y., Wang, Y.C., Zhen, Y.S., et al. (2019). An EGFR-targeting antibody-drug conjugate LR004-VC-MMAE: potential in esophageal squamous cell carcinoma and other malignancies. Mol. Oncol. *13*, 246–263.
38. Mullard, A. (2013). Maturing antibody-drug conjugate pipeline hits 30. Nat. Rev. Drug Discov. *12*, 329–332.
39. Sievers, E.L., and Senter, P.D. (2013). Antibody-drug conjugates in cancer therapy. Annu. Rev. Med. *64*, 15–29.
40. Beck, A., Goetsch, L., Dumontet, C., and Corvaïa, N. (2017). Strategies and challenges for the next generation of antibody-drug conjugates. Nat. Rev. Drug Discov. *16*, 315–337.
41. Sun, X., Ponte, J.F., Yoder, N.C., Laleau, R., Coccia, J., Lanieri, L., Qiu, Q., Wu, R., Hong, E., Bogalhas, M., et al. (2017). Effects of Drug-Antibody Ratio on Pharmacokinetics, Biodistribution, Efficacy, and Tolerability of Antibody-Maytansinoid Conjugates. Bioconjug. Chem. *28*, 1371–1381.
42. Lee, K.Y., Park, J.S., Jee, Y.K., and Rosen, G.D. (2002). Triptolide sensitizes lung cancer cells to TNF-related apoptosis-inducing ligand (TRAIL)-induced apoptosis by inhibition of NF-kappaB activation. Exp. Mol. Med. *34*, 462–468.

43. Xu, L., Qiu, Y., Xu, H., Ao, W., Lam, W., and Yang, X. (2013). Acute and subacute toxicity studies on triptolide and triptolide-loaded polymeric micelles following intravenous administration in rodents. Food Chem. Toxicol. *57*, 371–379.

44. Thurber, G.M., and Dane Wittrup, K. (2012). A mechanistic compartmental model for total antibody uptake in tumors. J. Theor. Biol. *314*, 57–68.

45. He, Q.L., Minn, I., Wang, Q., Xu, P., Head, S.A., Datan, E., Yu, B., Pomper, M.G., and Liu, J.O. (2016). Targeted Delivery and Sustained Antitumor Activity of Triptolide through Glucose Conjugation. Angew. Chem. Int. Ed. Engl. *55*, 12035–12039.

46. Zhang, K., Wang, J., Tong, T.R., Wu, X., Nelson, R., Yuan, Y.C., Reno, T., Liu, Z., Yun, X., Kim, J.Y., et al. (2017). Loss of H2B monoubiquitination is associated with poor-differentiation and enhanced malignancy of lung adenocarcinoma. Int. J. Cancer *141*, 766–777.

47. Zhang, X., Claerhout, S., Prat, A., Dobrolecki, L.E., Petrovic, I., Lai, Q., Landis, M.D., Wiechmann, L., Schiff, R., Giuliano, M., et al. (2013). A renewable tissue resource of phenotypically stable, biologically and ethnically diverse, patient-derived human breast cancer xenograft models. Cancer Res. *73*, 4885–4897.

48. Zhang, K., Keymeulen, S., Nelson, R., Tong, T.R., Yuan, Y.C., Yun, X., Liu, Z., Lopez, J., Raz, D.J., and Kim, J.Y. (2018). Overexpression of Flap Endonuclease 1 Correlates with Enhanced Proliferation and Poor Prognosis of Non-Small-Cell Lung Cancer. Am. J. Pathol. *188*, 242–251.

49. Zhang, K., Yang, L., Wang, J., Sun, T., Guo, Y., Nelson, R., Tong, T.R., Pangeni, R., Salgia, R., and Raz, D.J. (2019). Ubiquitin-specific protease 22 is critical to in vivo angiogenesis, growth and metastasis of non-small cell lung cancer. Cell Commun. Signal. *17*, 167.

50. Sutherland, M.S., Sanderson, R.J., Gordon, K.A., Andreyka, J., Cerveny, C.G., Yu, C., Lewis, T.S., Meyer, D.L., Zabinski, R.F., Doronina, S.O., et al. (2006). Lysosomal trafficking and cysteine protease metabolism confer target-specific cytotoxicity by peptide-linked anti-CD30-auristatin conjugates. J. Biol. Chem. *281*, 10540–10547.